Latin American Journal of Solids and Structures
www.lajss.org

Consideration of Spillover Effect in Active Vibration Suppression of a Smart Composite Plate Using Piezoelectric Elements

Abstract

In this paper, the problem of vibration suppression of a smart composite plate with bonded piezoelectric patches is considered. A higher order plate model is used for finite element modeling of the plate and the PID controller is used to generate control voltage command to the piezo actuators from the piezo sensors data. Derived formulation and the control algorithm is implemented in a finite element (FE) code and the FE modeling results are verified using available results of previous studies. The effect of control gain on the vibration suppression characteristics is studied. Furthermore, since FE modeling reduces the order of the real problem, the problem of un-modeled residual modes on the so-called spillover effect is investigated.

Keywords

Smart plate; finite element method; vibration suppression; piezoelectric; spillover.

Eman Eshraqi [a]
Morteza Shahravi [b]
Milad Azimi [c]

[a] Researcher, Malek Ashtar University of Technology, Tehran, Iran. eman.eshraqi@chmail.ir
[b] Malek Ashtar University of Technology, Tehran, Iran. Shahravi@aut.ac.ir
[c] Space Research Institute, Tehran, Iran. azimi.mld@gmail.com

http://dx.doi.org/10.1590/1679-78253089

Received 12.05.2016
In revised form 14.07.2016
Accepted 25.07.2016
Available online 03.08.2016

1 INTRODUCTION

In many practical applications, such as space satellites, it is important to control the shape or suppress the vibrations of a lightweight flexible structure. Thus the problems of dynamic analysis and vibration attenuation in flexible components of a spacecraft have been the subject of a number of researches (Azimi et al. 2015; Shahravi & Azimi 2015). Owing to direct and inverse piezoelectric effects, piezoelectric materials can produce electrical charges when they are subjected to mechanical loads, and thus can be used as sensors, or inversely produce strains when they are electrically excited, and thus used as actuators. They have been considered as one of the promising candidates to be used for active vibration control of light-weight structures. Considering the properties of piezoelectric materials, active vibration control of structural beams, plates and shells using embedded or surface bonded piezoelectric sensors and actuators has been investigated in many researches (Schulz et al. 2013; Vashist & Chhabra 2013; Wang et al. 2001; Wu et al. 2014). Considering the control of

piezoelectric smart structures, both conventional and modern control methods have been employed by various researchers. A survey on various control algorithms employed for vibration control of smart structures is presented in (Fei et al. 2010). Classical constant gain velocity feedback control (Farhadi & Hosseini-Hashemi 2011; He et al. 2004) and positive position feedback (PPF) (Baillargeon & Vel 2004) is widely employed for actively vibration control of piezoelectric smart beams and plates.

Investigating open literature reveals that in many studies, finite element (FE) modeling has been used to model the dynamic behavior of the structure (Xu & Koko 2004; Chandrashekhara & Agarwal 1993). In FE modeling of a plate using plate elements, the three-dimensional displacement field is reduced to a two-dimensional problem by adopting an appropriate formulation for variation of displacements across the thickness. Equivalent single layer and layer-wise theories are considered in approximating the displacement field of the structure to derive a reduced 2-D model instead of the complex 3-D model (Reddy 1993; Tornabene et al. 2013; Correia & Gomes 2000). A comprehensive research on various theories for displacement field modeling of composite structures with piezo-elements is given by (Benjeddou 2000).

A smart structure is a distributed parameter system with infinite degrees of freedom. Usually a reduced order model (ROM) with finite degrees of freedom pertaining to generalized coordinates is employed for design of a controller. A feedback controller based on a reduced model can destabilize the residual modes. In function of sensor position the feedback can excite the un-modeled state of system (control spillover), and the sensor signals are contaminated by the residual modes (observation spillover) and degrade the active vibration system efficiency (Dong et al. 2014; Jovanović et al. 2014). Some methods for reduction of spillover effects are discussed by (Mei & Mace 2002; Kim & Inman 2001).

This paper uses a higher order plate theory to derive a finite element model for vibration behavior of a composite plate with bonded piezoelectric patches. PID control algorithm is then used to investigate the vibration suppression characteristics of the piezo-actuators using gathered data of piezo-sensors. Effects of controller gain and the un-modelled dynamics in the controller design resulting in spillover effect is also studied.

2 FINITE ELEMENT MODELING

A sandwich plate of length L and width W is considered. The plate consists of a core layer of honeycomb structure with thickness t_c, which is sandwiched between two upper and lower face sheets of thicknesses t_u and t_l, respectively. The upper and lower face sheets are covered with piezoelectric patches and solar cells. The piezoelectric sensors/actuators have thickness of t_p and the solar cells have a thickness of t_s. A schematic of smart sandwich plate is shown in Fig. 1.

Higher order displacement field as given by (Correia & Gomes 2000), is considered to approximate the three-dimensional problem with a reduced two-dimensional plate model. The displacement field is given by (Correia & Gomes 2000):

$$u = u_0 + z\theta_{0x} + z^2 u_1 + z^3 \theta_{1x} \tag{1-a}$$

$$v = v_0 + z\theta_{0y} + z^2 v_1 + z^3 \theta_{1y} \tag{1-b}$$

$$w = w_0 + z\theta_{0z} + z^2 w_1 \tag{1-c}$$

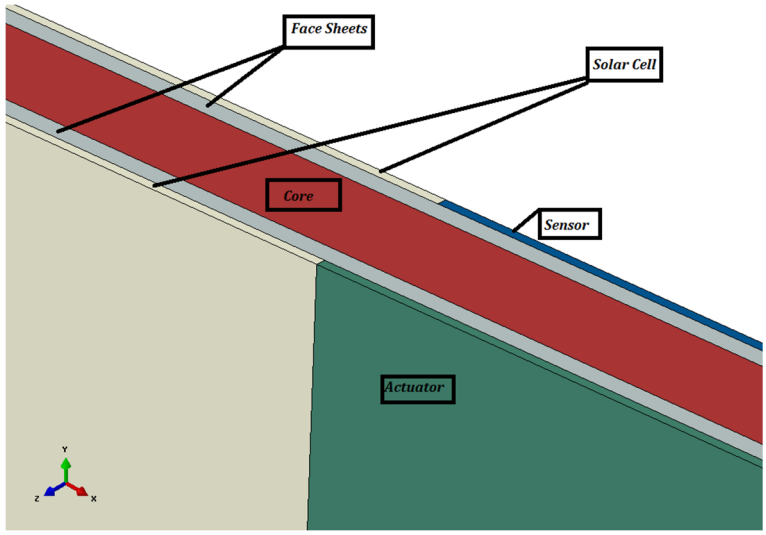

Figure 1: Schematic of smart sandwich plate.

Constitutive equations of the piezoelectricity can be written as (Correia & Gomes 2000):

$$\{\sigma\} = [C]\{\varepsilon\} - [e]\{E\} \tag{2-a}$$

$$\{D\} = [e^T]\{\varepsilon\} + [p]\{E\} \tag{2.b}$$

Where $\{\sigma\} = \{\sigma_{xx}\ \sigma_{yy}\ \sigma_{zz}\ \sigma_{xy}\ \sigma_{yz}\ \sigma_{xz}\}^T$ is the elastic stress vector and $\{\varepsilon\} = \{\varepsilon_{xx}\ \varepsilon_{yy}\ \varepsilon_{zz}\ \gamma_{xy}\ \gamma_{yz}\ \gamma_{xz}\}^T$ is the elastic strain vector. $[C]$ is the matrix of elastic coefficients and $[e]$ is the piezoelectric coefficients matrix. $\{D\} = \{D_x\ D_y D_z\}$ is the electric displacement vector and $[p]$ is the dielectric matrix. It is assumed that only the through thickness component of electric field vector is nonzero, thus $\{E\} = \{0\ 0\ E_z\}$, where E_z is given by:

$$E_z = -\frac{d\phi}{dz} \tag{3}$$

where ϕ is the electric potential across the thickness of the piezoelectric layer. Assuming linear variation of the electric potential through the piezo-layers thickness, due to their small thickness values, the electric field is given by $E_z = -\phi_\alpha / t_\alpha$, where α refers to a sensor or actuator piezo patch layer.

Following the procedure that is given in detail by (Correia & Gomes 2000), and using an eight-noded isoparametric element with eleven displacement degrees of freedom per node and additional one electric potential degree of freedom for each node, the finite element formulation for the dynamic governing equation of the smart sandwich plate in global form will be given as:

$$\begin{bmatrix} M_{dd} & 0 \\ 0 & 0 \end{bmatrix} \begin{Bmatrix} \ddot{d} \\ \ddot{\phi} \end{Bmatrix} + \begin{bmatrix} K_{dd} & K_{d\phi} \\ K_{\phi d} & K_{\phi\phi} \end{bmatrix} \begin{Bmatrix} d \\ \phi \end{Bmatrix} = \begin{Bmatrix} F_d(t) \\ F_\phi(t) \end{Bmatrix}, \tag{4}$$

where M_{dd} is the mass matrix and K_{dd} is the structural stiffness matrix, which include contributions from the core layer, face sheet layers, and solar cells and actuator patches. $K_{d\phi}$ and $K_{\phi d} = K_{d\phi}^T$ are the elastic-dielectric coupling matrices and $K_{\phi\phi}$ is the dielectric stiffness matrix, all of which contribute to the piezo patch layers. $\{d, \phi\}^T = \{u_0, v_0, w_0, \theta_{0x}, \theta_{0y}, \theta_{0z}, u_1, v_1, w_1, \theta_{1x}, \theta_{1y}, \phi\}^T$ is the unknown electro-mechanical nodal degrees of freedom. $F_d(t)$ is the mechanical nodal force vector and $F_\phi(t)$ is the nodal electric force vector. Details of elemental mass and stiffness matrices and the elemental force vectors that are assembled to form the global finite element matrices in Eq. (4) can be found in the work of (Correia & Gomes 2000) and are not repeated here for brevity.
The electric potential vector consists of sensory ϕ_S and actuator ϕ_A components. The electric voltage is only externally applied on the actuators. Thus it is possible to write Eq. (4) for sensors and actuators, separately:

$$[M_{dd}]\{\ddot{d}\} + [K_{dd}]\{d\} + \left[K_{d\phi}\right]_S\{\phi_S\} = \{F_d(t)\} - \left[K_{d\phi}\right]_A\{\phi_A\} \tag{5-a}$$

$$\left[K_{\phi d}\right]_A\{d\} + \left[K_{\phi\phi}\right]_A\{\phi_A\} = \left\{F_\phi(t)\right\}_A \tag{5-b}$$

$$\left[K_{\phi d}\right]_S\{d\} + \left[K_{\phi\phi}\right]_S\{\phi_S\} = \{0\} \tag{5-c}$$

Thus the induced electric potential of the sensors can be obtained from the last equation as:

$$\{\phi_S\} = -\left[K_{\phi\phi}\right]_S^{-1}\left[K_{\phi d}\right]_S\{d\} \tag{6}$$

where sub-indexes A and S refer to actuator part and sensor part of FE coupling stiffness matrices and electric vectors.

2.1 Static Analysis

For the static analysis, it is assumed that the structure is first deformed under the applied mechanical load and then the actuator control force is applied based on the sensor voltage which leads to additional deformation of the plate. The total deformation can be obtained from the superposition of two states as follows (Moita et al. 2004):

$$\{d\}^T = \{d\}^M + \{d\}^E \tag{7}$$

where $\{d\}^T$ is the total deformation of the plate and $\{d\}^M$ denotes deformation due to combination effects of applied external mechanical load and induced potential in the sensors and $\{d\}^E$ denotes deformation due to actuators voltage. Assuming that first $\{d\}^M$ occurs, the induced electric potentials in sensors can be obtained from Eq. (6) by substituting $\{d\} = \{d\}^M$. Substitution of the resulting expression for $\{\phi_S\}$ back in to Eq. (5-a) and disregarding inertia terms and actuator voltages, and putting $\{d\} = \{d\}^M$, $\{d\}^M$ can be obtained by solving the following equation (Moita et al. 2004):

$$\left([K_{dd}] - \left[K_{d\phi}\right]_S\left[K_{\phi\phi}\right]_S^{-1}\left[K_{\phi d}\right]_S\right)\{d\}^M = \{F_d\} \tag{8}$$

It is assumed that the actuator voltages are the amplified signals of sensors potentials, i.e. $\{\phi_A\} = -[G]\left[K_{\phi\phi}\right]_S^{-1}\left[K_{\phi d}\right]_S\{d\}^M$, where $[G]$ is a diagonal matrix of the amplifiers gains. Substitution of this expression for actuator voltages back in to Eq. (5-a), and considering the new induced

voltages in the sensors due to $\{d\}^E$, displacement due to actuating voltage $\{d\}^E$ can be determined from the solution of the following equation (Moita et al. 2004):

$$\left([K_{dd}] - [K_{d\phi}]_S [K_{\phi\phi}]_S^{-1} [K_{\phi d}]_S\right)\{d\}^E = [G][K_{d\phi}]_A [K_{\phi\phi}]_S^{-1} [K_{\phi d}]_S \{d\}^M \tag{9}$$

Total deformation can be obtained by solving Eqs. (8) and (9), and then substitution of the obtained results in Eq. (7).

2.2 Dynamic Analysis

Assuming that the converse piezoelectric effect is negligible for sensors, integration of electric displacement over the surface of each piezoelectric sensor element determines the output charge of that element as follows (Wang et al. 2001):

$$Q_j^i(t) = \frac{1}{2} \sum_{z=z_s^-, z_s^+} \int_{A_j} D_z(t) dA \tag{10}$$

where z_s^- and z_s^+ denote the lower and upper surfaces of the jth element of the ith electroplated sensor. The total charge of the ith sensor patch is then obtained by summation over all its constituents elements (Wang et al. 2001):

$$Q^i(t) = \Sigma Q_j^i(t) \tag{11}$$

Using the electro-mechanical coupling matrix of the jth element of the ith sensor patch, Eq. (10) can be re-written as:

$$Q_j^i(t) = [K_{\phi d}]_S^j \{d_j\} \tag{12}$$

where $\{d_j\}$ is the nodal displacement vector of jth element. The total electric charge on the ith sensor can be obtained by assembling the electric charges of all elements in the ith sensor due to Eq. (11), which gives:

$$Q^i(t) = [K_{\phi d}]_S^i \{d\} \tag{13}$$

Piezoelectric sensors are considered to measure the strain rate, thus the output voltage is given by:

$$\Phi_S^i = G_i^s \frac{dQ_i}{dt} = G_i^s [K_{\phi d}]_S^i \{\dot{d}\} \tag{14}$$

where G_i^s is the gain of charge amplifier of the ith sensor. Considering N_s total sensors bonded to the smart sandwich plate, the sensor voltage vector can be expressed as:

$$\{\Phi_S\} = \left[\Phi_S^1 \dots \Phi_S^{N_s}\right]^T = [G^s][K_{\phi d}]_S \{\dot{d}\} \tag{15}$$

where $[G^s]$ is diagonal and $[K_{\phi d}]_S$ is formed by assembling all the corresponding electro-elastic coupling matrices of all sensors.

For the purpose of vibration suppression, the error signal is considered to be the potential of the sensors which should be set to zero by applying appropriate actuating voltages. A PID controller is assumed to produce the required voltage of actuators from the output voltage of the sensors as (Rahman & Alam 2012):

$$\{\Phi_a\} = [G_p]\{\Phi_s\} + [G_i]\int \{\Phi_s\}\, dt + [G_d]\{\dot{\Phi}_s\} \tag{16}$$

It is assumed that each sensor patch is accompanied by a corresponding actuator patch with a unique gain. Thus using Eq. (15) it is possible to write:

$$\{\Phi_a\} = [K_p][K_{\phi d}]_S\{\dot{d}\} + [K_i][K_{\phi d}]_S\{d\} + [K_d][K_{\phi d}]_S\{\ddot{d}\} \tag{17}$$

where $[K_p]$, $[K_i]$, and $[K_d]$ are diagonal matrices of product of PID gains and sensor gains. Substitution of Eq. (17) into the first relation of Eq. (5), the governing equations of the motion of the system with active damping can be derived as:

$$([M_{dd}] + [M_A])\{\ddot{d}\} + ([C_S] + [C_A])\{\dot{d}\} + \left([K_{dd}] - [K_{d\phi}]_S[K_{\phi\phi}]_S^{-1}[K_{\phi d}]_S + [K_A]\right)\{d\} = \{F_d(t)\} \tag{18}$$

where $[C_S] = \alpha[M_{dd}] + \beta[K_{dd}]$ is the structural damping with α and β being the Rayleigh type damping coefficients. $[M_A]$, $[C_A]$, and $[K_A]$ are respectively the active control mass, damping, and stiffness effects given by:

$$[M_A] = [K_{d\phi}]_A[K_d][K_{\phi d}]_S \tag{19}$$

$$[C_A] = [K_{d\phi}]_A[K_p][K_{\phi d}]_S \tag{20}$$

$$[K_A] = [K_{d\phi}]_A[K_i][K_{\phi d}]_S \tag{21}$$

Eq. (18) can be solved using a direct integration scheme such as the Newmark method (Bathe & Wilson 1976). The PID controller parameters can be obtained using a suitable method such as Ziegler-Nicholes.

3 VERIFICATION STUDIES

Two numerical examples are considered to assess the accuracy of the developed formulation. In the first example a cantilever bimorph Kynar piezoelectric beam is considered. The upper layer is polarized in the direction of applied voltage and the bottom layer has the opposite polarization. The material properties of the Kynar layer are given in (Shakeri et al. 2009). The effect of applied voltage on the deflection of the free end of the beam is investigated by (Koconis et al. 1994) and are compared with the present study results in Fig. 2. Good agreement is seen between the numerical results of current study with the experimental results of (Koconis et al. 1994).

In the second example a cantilever bimorph piezoelectric beam with the ratio of length to thickness $L/h = 6$ is considered. The beam is considered to consist of two PZT layers with opposite polarization directions and its material properties are given by:

$$\begin{gathered} c_{11} = 60.6\ (\mathrm{GPa});\ c_{55} = 23.0\ (\mathrm{GPa}); \\ d_{31} = -274\times10^{-12}\ (\mathrm{CN}^{-1}) \\ \rho = 7500\ (\mathrm{kg/m}^3) \end{gathered} \tag{22}$$

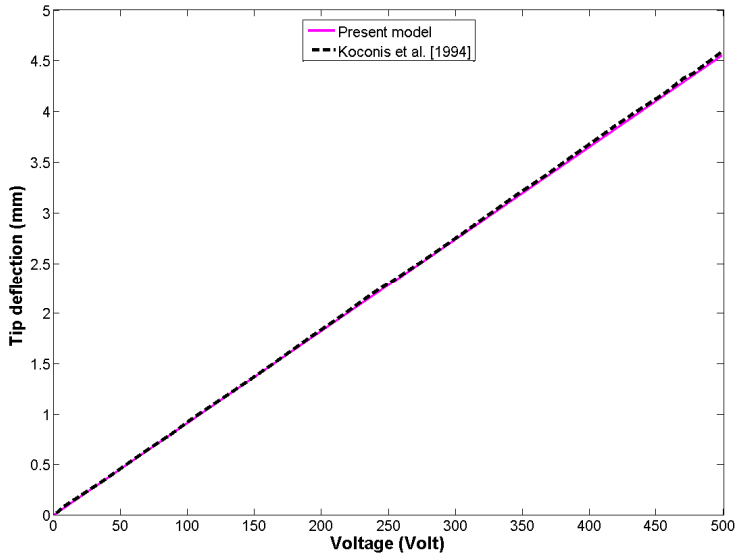

Figure 2: Comparison of the results of free end deflection of a cantilevered bimorph Kynar beam under applied voltage.

Exact results for the free end deflection of the beam under two loading conditions including (a) applied uniformly distributed load of $q = 100\ (\mathrm{kN/m^2})$ and (b) applied voltage of $V = 100\ (\mathrm{V})$ are given by (Yang & Xiang 2007). The first natural frequency of the beam is also reported in (Lee et al. 2005). These values are compared in table 1 with results of current study derived with FE modeling.

Free end deflection (m)		
Loading type	Exact (Yang & Xiang 2007)	Present model
$q = 10\ (\mathrm{kN/m^2})$	3.286×10^{-4}	3.286×10^{-4}
$V = 100\ (\mathrm{V})$	14.796×10^{-7}	14.796×10^{-7}
First natural frequency (Hz)		
(Lee et al. 2005)	12.574	
Present model	12.514	

Table 1: Comparison of the results of free end deflection and first natural frequency for a bimorph piezoelectric beam.

4 NUMERICAL RESULTS

Verifying the FE model and the corresponding numerical implementation, active control of a smart sandwich plate is described in this section. A square sandwich plate of length $L = 400\ (mm)$ fixed

at one of its edges and free to vibrate at other edges is considered in this section. The plate consists of an aluminum honeycomb core structure with two face-sheets attached above and below of the core layer which are also made from aluminum. A zig-zag combination of sensor/actuator pairs are located on the face-sheets as shown in Fig. 3. The rest of the surfaces of the sandwich plate is covered with solar cells. Geometric properties and electro-mechanical properties of each layer of the smart plate are given in table 2 and table 3, respectively.

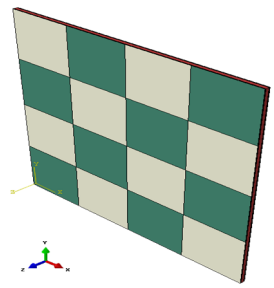

Figure 3: Sandwich plate configuration with zig-zag placement of piezo patches.

Component	Thickness (mm)	Width (mm)	Length (mm)
Core	5	400	400
Face-sheets	1	400	400
Sensors	0.5	100	100
Actuators	0.5	100	100
Solar cells	0.5	100	100

Table 2: Geometric characteristics of the smart sandwich plate.

Component	Mechanical properties	Density ($\mathrm{kg/m^3}$)	Electrical properties
Core	$E_x = E_y = E_z = 68.9\ (\mathrm{GPa})$ $G_{xz} = 5.2\ (\mathrm{GPa})$ $G_{yz} = 13.4\ (\mathrm{GPa})$ $\nu = 0.33$	2768	-
Face-sheets	$E = 68.9\ (\mathrm{GPa})$ $\nu = 0.33$	$2768\ \mathrm{kg/m^3}$	-
Piezo actuators and sensors	$E = 69\ (\mathrm{GPa})$ $\nu = 0.3$	$7700\ \mathrm{kg/m^3}$	$e_{31} = e_{32} = -12.5\ (\mathrm{C/m^2})$ $p = 1.6\times10^{-8}\ (\mathrm{C/Vm})$
Solar cells	$E = 81.3\ (\mathrm{GPa})$ $\nu = 0.29$	$7500\ \mathrm{kg/m^3}$	-

Table 3: Electro-mechanical properties of various layers of the smart sandwich plate.

To investigate the accuracy of developed mesh and FE analysis, a finite element model of the sandwich plate is also developed in the ABAQUS commercial code environment. Transverse deflec-

tion of the line $y = 200\ (mm)$ when the plate is subjected to a uniform distributed mechanical load of $q = 1\ (N/m^2)$ and applied voltage of $V = 1\ (V)$ are shown in Figs. 4 and 5, respectively.

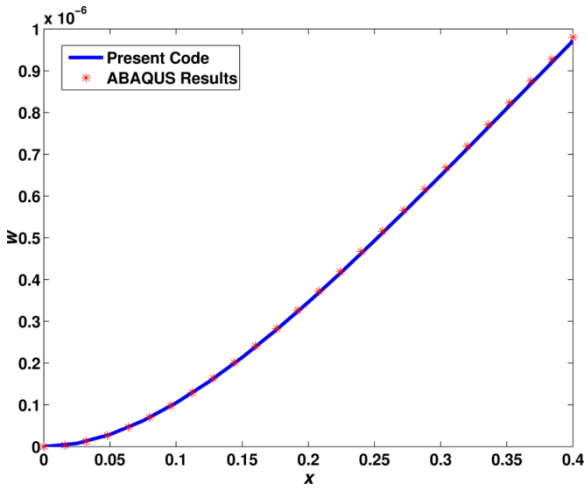

Figure 4: Transverse deflection of the line $y = 200\ (mm)$ when the plate is subjected to uniform distributed load.

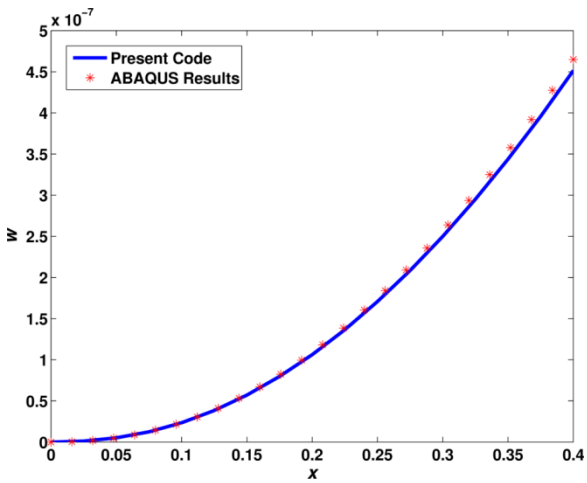

Figure 5: Transverse deflection of the line $y = 200\ (mm)$ when the actuators are subjected to uniform electric voltage.

The first five natural frequencies of the plate obtained from FE analysis based on the theory used in this study is compared with the results obtained from ABAQUS simulation in table 4.

	Natural Frequency (Hz)				
	Mode 1	Mode 2	Mode 3	Mode 4	Mode 5
Present results	38.6	93.1	236.0	302.2	340.0
ABAQUS simulation	38.4	92.3	233.1	298.1	335.2

Table 4: Comparison of the results of present FE analysis with natural frequencies extracted from ABAQUS.

First to third mode-shapes extracted from current FE analysis to those obtained from FE simulation in ABAQUS are also compared in Fig 6 (a)-(c).

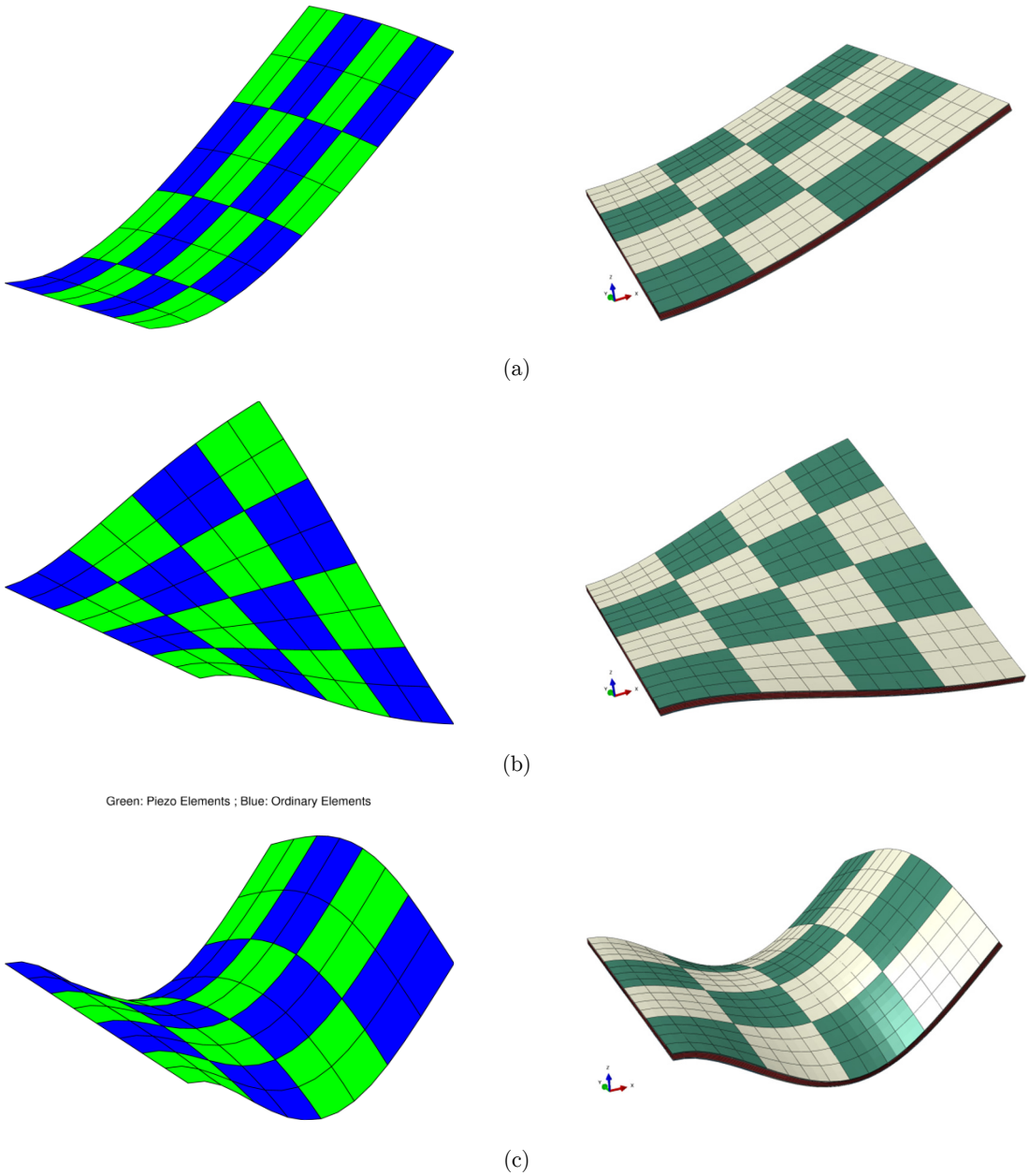

Figure 6: Sandwich plate mode shapes of free vibration (Left: Present FE analysis, Right: ABAQUS simulation) (a) mode 1, (b) mode 2, and (c) mode 3.

Transient deflection of the mid-node of the plate at the free end ($x = 400\,(mm), y = 200\,(mm)$) when the plate is subjected to the time-varying uniformly distributed load shown in Fig.

7 (b) is obtained from FE analysis and simulation in ABAQUS. The results are compared in Fig. 7 (a) for a time period of $t = 0.3\ (s)$.

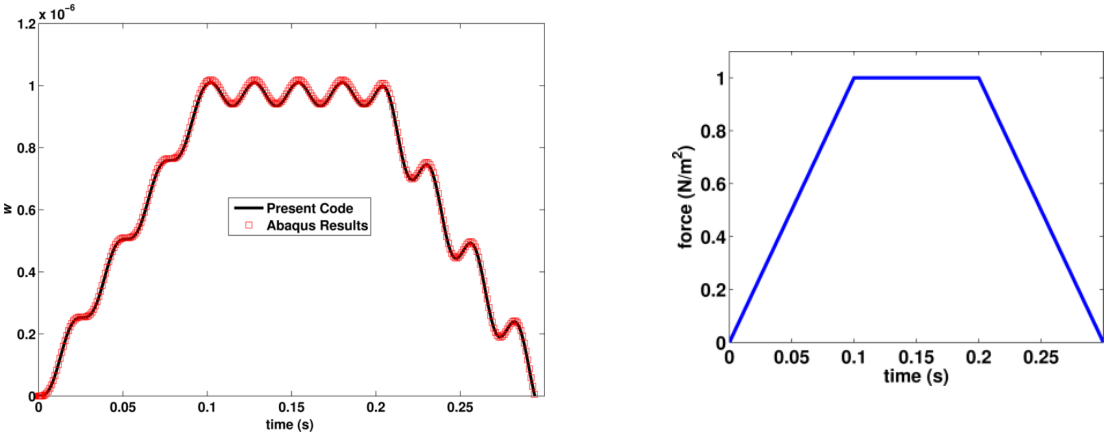

(a) (b)

Figure 7: Transient deflection of the mid-node at the free end (a) when the plate is subjected to a transient uniform load shown in (b).

The performance of the PID controller in damping the transverse vibrations of the plate corresponding to its first mode of vibration is investigated in Fig. 8. The plate is initially bent by applying a uniformly distributed load of $q = 1\ N/m^2$, and then removing the load, making the plate to vibrate at its first natural frequency. The displacement history of the mid-node located at the free edge of the plate at $x = X_L$ is used to measure the performance of the PID controller. Structural damping is neglected. It is observed that the PID controller is able to reduce the vibrations of the plate and make the steady-state response equal to zero. Variation of piezoelectric actuator voltage for the piezo-patch with its centroid located at $x = L/8$ and $y = 5L/8$, is shown in Fig. 9. The piezoelectric actuator voltage tends to zero as the time increases.

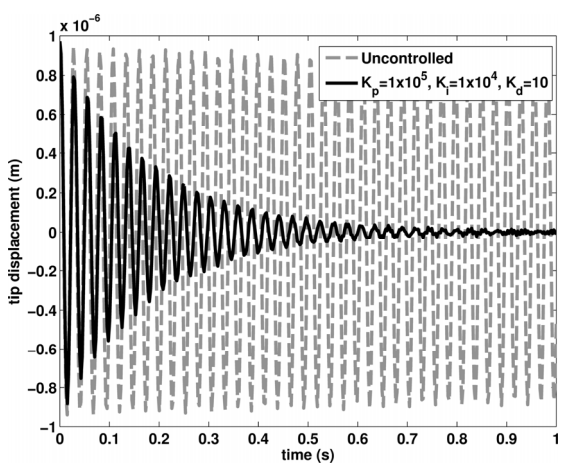

Figure 8: Deflection of the middle node located at the free edge of the plate.

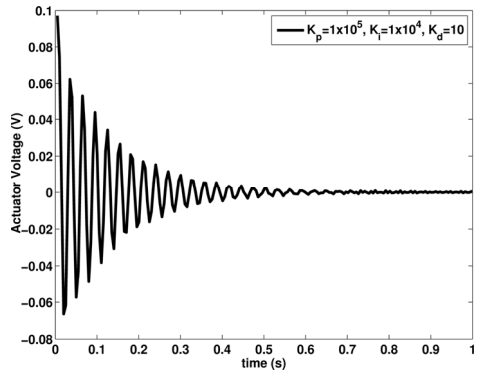

Figure 9: Variation of actuator voltage with time.

5 THE SPILLOVER EFFECT

Flexible smart structures are distributed parameters systems which have infinite degrees of freedom. Active vibration control design usually requires a mathematical model of the structure which is at best a reduced model with finite degrees of freedom. A feedback controller designed based upon a reduced model may stimulate the residual modes (un-modeled dynamics) and make the structure unstable. Due to the sensor location a feedback signal may excite the un-modeled dynamics of the structure or the sensor signals may be contaminated with the residual modes. These are referred to control spillover and observation spillover, respectively.

For the PID controller considered in this study, it has been observed that increasing the PID gains have two effects. First, increasing the controller gains results in reduction of the amplitude of vibrations pertaining to the first mode, which is expected since the controller is designed based on vibration suppressions of the first mode. The second effect is that increasing the PID gains results in appearance of vibrations pertaining to higher modes of structural vibration. Since the feedback control leads to excitement of un-modeled states, the performance of the controller is affected by the spillover, when the gains are increased. This can be clearly seen when investigating the response of the smart plate by increasing the derivational gain as shown in Fig. 10. A similar unstability in the voltage of the actuator is also observed as Fig. 11 indicates. As can be seen from this figure, the voltage does not tend to zero as expected and it diverges to higher values with time.

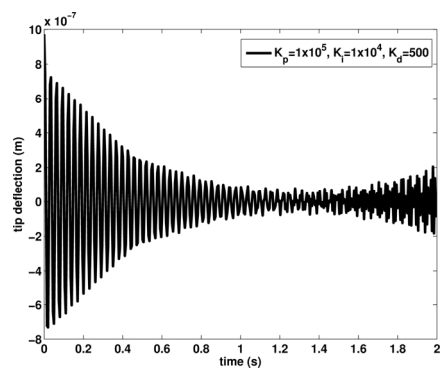

Figure 10: Effect of increasing the derivative gain on the deflection of the middle node located at the free edge of the plate.

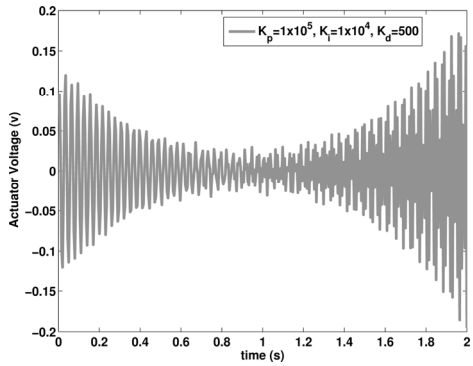

Figure 11: Effect of increasing the derivative gain on the actuator voltage history.

6 CONCLUSIONS

The problem of vibration control of a smart sandwich plate with bonded piezoelectric patches was considered in this study. A higher order plate model was adopted for displacement field variation across the plate thickness. A PID control algorithm was employed to convert sensor signals into actuator voltages. A FE code was written based on the derived formulation incorporating the control algorithm in the transient analysis of the plate.

Verification studies were performed to investigate the accuracy of the developed FE formulation and the written code, and good correspondence was seen to exist between the results of the FE analysis based on higher-order 2-D formulation with the available results in the literature and the results of FE simulations by ABAQUS. Thus, it was shown that the developed model can accurately predict the deflection of the plate under mechanical and electrical loads. The control algorithm was successfully employed to attenuate the flexural vibrations of the smart plate corresponding to its first mode shape. The spillover effect was shown to intensify by increasing the derivative gain of the PID controller. To minimize the spillover effects, it is suggested to optimally place the piezo actuators and sensors on the plate surface.

References

Azimi, M., Shahravi, M., Joubaneh, E. (2015). Dynamic analysis of maneuvering flexible spacecraft appendage using higher order sandwich panel theory, Latin American Journal of Solids and Structures 13: 296–313.

Baillargeon, B. P., Vel, S. S. (2004). Active Vibration Suppression of Sandwich Beams using Piezoelectric Shear Actuators, Advances in Computational & Experimental Engineering & Science 16: 2093–2098.

Bathe, K., Wilson, E. L. (1976). Numerical methods in finite element analysis, Prentice-Hall, Englewood Cliffs, NJ.

Benjeddou, A. (2000). Advances in piezoelectric finite element modeling of adaptive structural elements: a survey, Computers and Structures 76: 347–363.

Chandrashekhara, K., Agarwal, A. (1993). Active vibration control of laminated composite plates using piezoelectric devices: a finite element approach, Journal of Intelligent Material Systems and Structures 4: 496–508.

Correia, V., Gomes, M. (2000). Modelling and design of adaptive composite structures, Computer Methods in Applied Mechanics and Engineering 185: 325–346.

Dong, X., Peng, Z., Zhang, W., Hua, H.X., Meng, G. (2014). Research on spillover effects for vibration control of piezoelectric smart structures by ANSYS, Mathematical Problems in Engineering, 2014: Article ID 870940, 8 pages.

Farhadi, S., Hosseini-Hashemi, S. H. (2011). Active vibration suppression of moderately thick rectangular plates, Journal of Vibration and Control, 17: 2040–2049.

Fei, J., Fang, Y., Yan, C. (2010). The Comparative study of vibration control of flexible structure using smart materials, Mathematical Problems in Engineering, 2010: Article ID 768256, 13 pages.

He, X. Q., Ng, T. Y., Sivashanker, S., Liew, K. M. (2001). Active control of FGM plates with integrated piezoelectric sensors and actuators, International Journal of Solids and Structures 38: 1641–1655.

Jovanović, M. M., Simonović, A. M., Zorić, N. D., Lukić, N. S., Stupar, S. N., Petrović, A. S., Wei, L. (2014). Experimental investigation of spillover effect in system of active vibration control, FME Transactions 42: 329–334.

Kim, M. H., Inman, D. J., (2001). Reduction of observation spillover in vibration suppression using a sliding mode observer, Journal of Vibration and Control 7: 1087–1105.

Koconis, D. B., Kollár, L. P., Springer, G. S. (1994). Shape control of composite plates and shells with embedded actuators. I. Voltages specified, Journal of Composite Materials 28: 415–458.

Lee, S. Y., Ko, B., Yang, W. (2005). Theoretical modeling, experiments and optimization of piezoelectric multimorph, Smart Materials and Structures 14: 1343–1352.

Mei, C., Mace, B. R. (2002). Reduction of control spillover in active vibration control of distributed structures using multioptimal schemes, Journal of Sound and Vibration 251: 184–192.

Moita, J. M. S., Correia, I. F., Soares, C. M. M., Soares, C. A. M. (2004). Active control of adaptive laminated structures with bonded piezoelectric sensors and actuators, Computers & Structures, 82: 1349–1358.

Rahman, N., Alam, M. N. (2012). Active vibration control of a piezoelectric beam using PID controller: Experimental study. Latin American Journal of Solids and Structures, 9: 657–673.

Reddy, J. N. (1993). An evaluation of equivalent-single-layer and layerwise theories of composite laminates, Composite Structures 25: 21–35.

Schulz, S. L., Gomes, H. M., Awruch, A. M. (2013). Optimal discrete piezoelectric patch allocation on composite structures for vibration control based on GA and modal LQR, Computers & Structures 128: 101–115.

Shahravi, M., Azimi, M. (2015). A comparative study for collocated and non-collocated sensor/actuator placement in vibration control of a maneuvering flexible satellite, Proceedings of the Institution of Mechanical Engineers, Part C: Journal of Mechanical Engineering Science 229: 1415–1424.

Shakeri, M., Sadeghi, S. N., Javanbakht, M., Hatamikian, H. (2009). Dynamic analysis of functionally graded plate integrated with two piezoelectric layers, based on a three-dimensional elasticity solution, Proceedings of the Institution of Mechanical Engineers, Part C: Journal of Mechanical Engineering Science 223: 1297–1309.

Tornabene, F., Viola, E., Fantuzzi, N. (2013). General higher-order equivalent single layer theory for free vibrations of doubly-curved laminated composite shells and panels, Composite Structures 104: 94–117.

Vashist, S. K., Chhabra, D. (2014, March). Optimal placement of piezoelectric actuators on plate structures for active vibration control using genetic algorithm, In SPIE Smart Structures and Materials+ Nondestructive Evaluation and Health Monitoring (905720-905720), International Society for Optics and Photonics.

Wang, S. Y., Quek, S. T., Ang, K. K. (2001). Vibration control of smart piezoelectric composite plates, Smart materials and Structures 10: 637–644.

Wu, D., Huang, L., Pan, B., Wang, Y., Wu, S. (2014). Experimental study and numerical simulation of active vibration control of a highly flexible beam using piezoelectric intelligent material, Aerospace Science and Technology 37: 10–19.

Xu, S. X., Koko, T. S. (2004). Finite element analysis and design of actively controlled piezoelectric smart structures, Finite Elements in Analysis and Design, 40: 241–262.

Yang, J., Xiang, H. J. (2007). Thermo-electro-mechanical characteristics of functionally graded piezoelectric actuators, Smart Materials and Structures 16: 784–797.